Spontaneous Oscillations and Waves during Chemical Vapor Deposition of InN

F. Jiang,[1,*] A. Munkholm,[2] R.-V. Wang,[1,3,+] S. K. Streiffer,[3] Carol Thompson,[4] P. H. Fuoss,[1] K. Latifi,[4] K. R. Elder,[5] and G. B. Stephenson[1,3,‡]

[1]*Materials Science Division, Argonne National Laboratory, Argonne, Illinois 60439, USA*
[2]*Philips Lumileds Lighting Company, San Jose, California 95131, USA*
[3]*Center for Nanoscale Materials, Argonne National Laboratory, Argonne, Illinois 60439, USA*
[4]*Department of Physics, Northern Illinois University, DeKalb, Illinois 60115, USA*
[5]*Department of Physics, Oakland University, Rochester, Michigan 48309, USA*

(Received 18 May 2008; published 22 August 2008)

We report observations of self-sustaining spatiotemporal chemical oscillations during metal-organic chemical vapor deposition of InN onto GaN. Under constant supply of vapor precursors trimethylindium and NH_3, the condensed-phase cycles between crystalline islands of InN and elemental In droplets. Propagating fronts between regions of InN and In occur with linear, circular, and spiral geometries. The results are described by a model in which the nitrogen activity produced by surface-catalyzed NH_3 decomposition varies with the exposed surface areas of GaN, InN, and In.

DOI: 10.1103/PhysRevLett.101.086102 PACS numbers: 68.55.ag, 81.05.Ea, 82.33.Ya, 82.40.Ck

Studies of spatiotemporal pattern formation in reaction-diffusion systems promise not only to provide models for complex phenomena such as organization and dynamics in living systems, but also to suggest new synthesis strategies for advanced materials [1]. Self-sustaining spatiotemporal chemical oscillations have been reported in several widely different types of excitable media, including reactions in solution [2,3], molecular reactions on surfaces [3–5], electrochemical systems [6,7], amoeba colonies [8], and cardiac muscle [9]. The nonlinear behavior of these systems is driven by positive feedback between coupled processes, often involving catalyzed reactions, and the resulting complex dynamics is a vibrant field of study [10–15].

A developing area in nonequilibrium science is the synthesis of metastable materials such as InN [16]. This semiconductor has the smallest bandgap of group III nitrides [17] and promises high mobility and saturation carrier velocity [18]. It has, however, been difficult to synthesize InN of high structural quality. Being the least stable of the group III nitrides, InN growth requires a high nitrogen activity equivalent to $\sim 10^3$ bar of N_2 at typical growth temperatures [19]. For the metal-organic chemical vapor deposition (MOCVD) process, decomposition of NH_3 is used to provide a chemically active nitrogen species. Complex growth behavior has been observed [20,21] and the molecular mechanisms are not well understood.

Here we report that self-sustaining oscillations can occur in MOCVD growth of InN onto GaN. Figure 1 shows oscillations in x-ray signals during growth under constant input flows, due to a cyclic process: islands of crystalline InN nucleate and grow; the InN islands collectively transform into elemental In droplets; the liquid In evaporates; and then another cycle of InN growth begins. Propagating fronts with linear, circular, and spiral geometries occur. The observed behavior is qualitatively explained by a model in which the effective nitrogen activity produced during catalytic decomposition of NH_3 at the substrate depends on the exposed surface areas of GaN, InN, and In. This phenomenon not only opens up a new class of excitable media involving transformations between vapor and bulk condensed phases for fundamental studies of nonlinear dynamics, but also provides insight into the nature of the chemical mechanisms involved in synthesis of metastable materials such as InN.

Our primary experimental approach is to use *in-situ* synchrotron x-ray diffraction and fluorescence during MOCVD growth to observe in real time the crystal structure and composition of the material deposited onto a substrate [22,23]. MOCVD is an example of a reaction in an open system, since vapor reactants are supplied and vapor by-products are exhausted continuously. We use

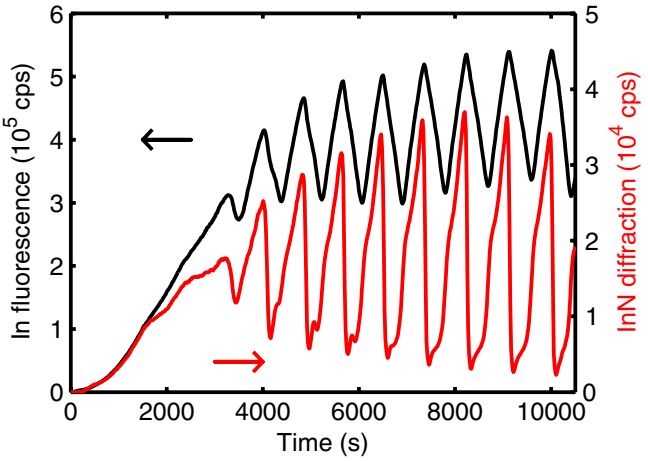

FIG. 1 (color online). Indium fluorescence and InN (110) diffraction intensities versus time after initial injection of $p(\mathrm{TMI}) = 1.22 \times 10^{-3}$ mbar at 937 K, $p(NH_3) = 40$ mbar.

epitaxial GaN (0001) films on sapphire as the substrate, and trimethylindium (TMI) as the In source. We observe that crystals of InN or droplets of elemental In [24] can be deposited when the TMI partial pressure p(TMI) exceeds a respective threshold. If p(TMI) is lowered below the threshold, the deposited material evaporates. These phase boundaries as a function of temperature are detailed in supplementary material [23]. At lower substrate temperatures (e.g. $T < 975$ K at NH_3 partial pressure $p(NH_3) = 40$ mbar), the threshold for depositing InN is lower than that for elemental In. The intensity of InN Bragg diffraction is used to monitor the amount of InN present on the surface, while the intensity of In $K\alpha$ x-ray fluorescence gives the total amount of both InN and elemental In.

The oscillatory behavior shown in Fig. 1 occurs when the GaN substrate is exposed to constant p(TMI) and $p(NH_3)$ under conditions where InN initially forms but elemental In evaporates. After initial InN nucleation and growth, spontaneous oscillations develop. The InN diffraction signal repeatedly rises to a maximum and then falls suddenly. The time of this sudden drop corresponds to the maximum in the In fluorescence, but the In fluorescence falls more slowly than the InN diffraction. Thus crystalline InN transforms into elemental In liquid at that point in the cycle. The lattice parameters of the InN islands remain equal to their stress-free bulk values throughout the process. This oscillatory system differs qualitatively from those previously reported (e.g. molecular surface reactions such as CO oxidation on Pt [3–5]) since we observe reactions and phase transformations between vapor species and condensed-phase particles.

The x rays illuminate a small region in the center of the substrate. To investigate whether the observed oscillations are due to spatial pattern formation on a larger scale, we have imaged the complete substrate area during growth using scattered visible light. We indeed find spatiotemporal waves of various types, as shown in Fig. 2. Linear waves, expanding circular disks, or expanding spirals form depending on boundary conditions. The velocity of a typical wave front such as that in Figs. 2(a) and 2(b) is $\sim 2.5 \times 10^{-3}$ cm/s. Video clips of the propagation of these waves are available online [23]. Because the oscillation periods observed were typically $\sim$1000 s, the sample could be quenched for *ex situ* study by turning off TMI flow and lowering the temperature as rapidly as possible (0.7 K/s), with little change in the x-ray signals (apart from crystallization of the liquid In). Figure 3 shows atomic force microscopy images of faceted hexagonal InN islands and of spherical (solidified) In droplets, taken from regions on opposite sides of a transformation wave front. Light scattering from these particles produces the contrast in Fig. 2, in which dark regions correspond to InN and light regions to elemental In. Figure 4(a) shows the sequence of transformations that occurs when stable periodic oscillations have developed. The amount of crystalline InN on the surface is proportional to the diffraction intensity, and the total amount of InN and elemental In liquid is proportional to the In fluorescence intensity. The intensities have been normalized so that the difference gives the amount of elemental In liquid. At the maximum in the fluorescence, the InN converts into elemental In, while at the minimum, the elemental In converts into InN. The fluorescence intensity oscillates because InN particles grow from the vapor during one half of the cycle, while In droplets evaporate during the other half.

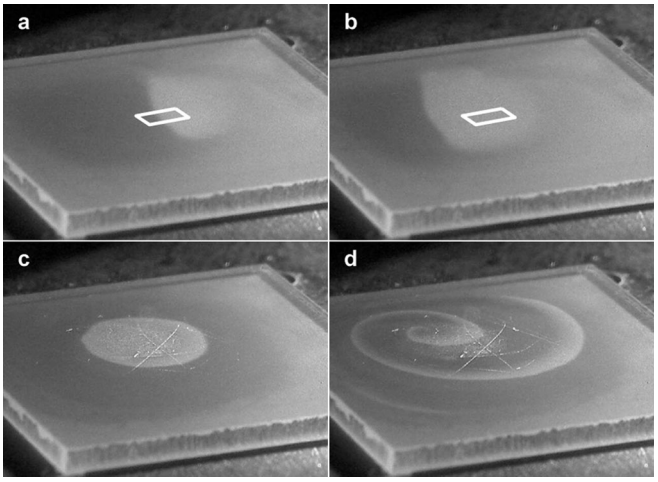

FIG. 2. Optical images of a 15×15 mm substrate during growth on its central area at 937 K. Regions of InN islands and In droplets correspond to dark and light contrast, respectively. (a) and (b) Recorded with Fig. 1 data at times 8262 and 8342 s, showing wave moving from right to left; p(TMI) $= 1.22 \times 10^{-3}$ mbar, $p(NH_3) = 40$ mbar. White outline shows x-ray illuminated area. (c) Expanding circular disk; p(TMI) $= 0.92 \times 10^{-3}$ mbar, $p(NH_3) = 40$ mbar. (d) Outwardly propagating spiral; p(TMI) $= 1.22 \times 10^{-3}$ mbar, $p(NH_3) = 57$ mbar.

We have investigated the behavior under different conditions of p(TMI), $p(NH_3)$, and substrate temperature. Oscillations develop over the entire region in which InN initially condenses but elemental In evaporates [23].

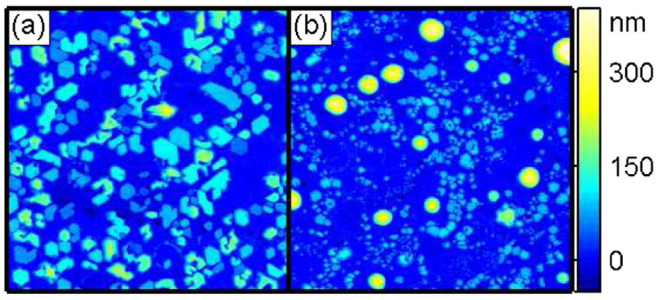

FIG. 3 (color online). Atomic force microscopy images of (a) hexagonal InN islands and (b) spherical elemental In droplets on a sample quenched after $\sim$5 oscillation periods under the same conditions as data shown in Fig. 1. (10×10 μm areas).

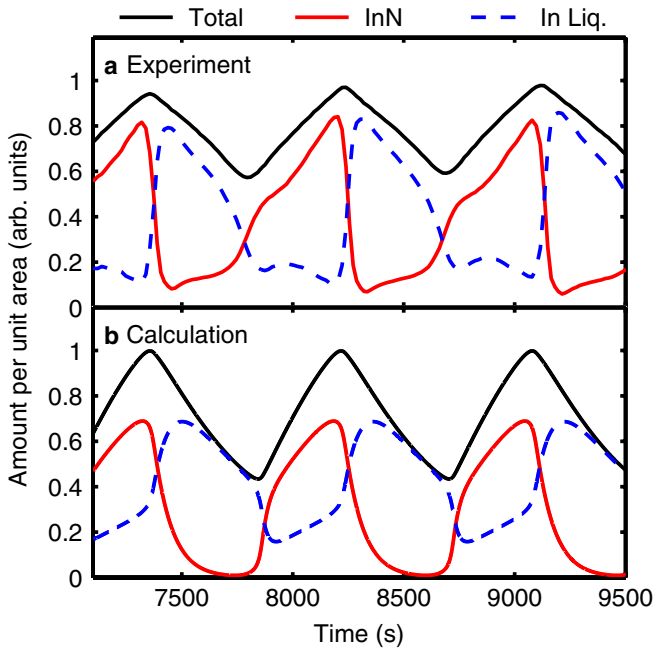

FIG. 4 (color online). (a): Total (InN + In Liquid) and InN curves are normalized fluorescence and diffraction data from Fig. 1; In Liquid curve is the difference. (b): Calculated Total, InN, and In Liquid evolution from reaction-diffusion model. Parameter values used are $q = 0.5$, $r = 1$, $k_1 = 0.05$, $k_2 = 0.40$, $k_3 = 2$, $\gamma_2/\gamma_1 = 2$, $\gamma_3/\gamma_1 = 0.08$, and $\gamma_1 = 0.0147\ \mathrm{s}^{-1}$.

Slower linear, circular, or spiral wave propagation occurs at lower p(TMI) within this region, while faster, increasingly chaotic behavior occurs at higher p(TMI). We have also carried out measurements using sapphire substrates without GaN films. While a region of initial InN condensation is found, no sustained oscillations are observed, indicating that the nature of the substrate is involved in the oscillatory mechanism.

Cyclic interconversion of micron-size particles of InN and elemental In at constant pressure and temperature implies that the effective nitrogen chemical potential oscillates with time. Since this is determined by the chemically active nitrogen species produced as intermediates in the catalytic decomposition of NH_3 to N_2 on the surface [25], this process is key to understanding the oscillatory behavior. Changes in the nature of the surface (such as coverage of GaN by InN and In) will affect the rates of creation or annihilation of the active species, modifying its concentration despite a constant supply of NH_3. Based on the hypothesis that the nitrogen activity p produced by NH_3 decomposition is highest for GaN surfaces and lowest for elemental In liquid, we propose the following oscillatory mechanism: (a) InN islands initially grow from vapor TMI under the high p from NH_3 decomposition on the exposed GaN surface. (b) An instability to transformation of the InN islands into elemental In droplets develops, where initial transformation decreases p, accelerating the process. (c) The In droplets begin to evaporate, exposing GaN surface. (d) The resulting increased p allows InN to grow again, initially by converting the remaining In droplets and then using incoming TMI vapor. This cycles back to (b).

We have developed a preliminary mathematical model [23] for this mechanism using a set of coupled equations describing the evolution of the amounts of the condensed phases InN, x, and elemental liquid In, y,

$$\dot{x} = \gamma_1(pq - k_1 x) + \gamma_2(py - k_2 x), \tag{1}$$

$$\dot{y} = \gamma_2(k_2 x - py) + \gamma_3(q - k_3 y), \tag{2}$$

where the coefficients γ_i and k_i give the rate and equilibrium constants of reaction, and q is the activity of In supplied by the vapor. In Eq. (1) the two terms give the net rate of InN formation from In vapor and In liquid, respectively. The two terms in Eq. (2) are the net rate of In liquid formation from InN and In vapor, respectively. Equations (1) and (2) describe averages over macroscopic length scales only, not the variations at the length scale of individual islands or droplets.

While the coefficients γ_i, k_i, and the In vapor activity, q, are taken to be constant in Eqs. (1) and (2), the nonlinearity that produces oscillatory behavior comes from the dependence of the N activity p on the amounts of the condensed phases x and y. It can be modeled by the rate equation [23]

$$\dot{p} = \gamma_4(x, y)r - \gamma_5(x, y)p^2 + D\nabla^2 p, \tag{3}$$

where r is the (constant) concentration of NH_3. The three terms give the rate of active nitrogen species (N^*) formation from NH_3, the rate of N^* loss to form inactive N_2, and transport of N^*, respectively. If γ_4 and γ_5 are large compared with γ_i in Eqs. (1) and (2) and transport is neglected, the value of p rapidly follows the changes in x and y, with $p^2 \approx r\gamma_4/\gamma_5$. To model the behavior observed, p should be maximum when no condensed In is present ($y = 0$). In calculations shown here we have used $p = r^{1/2}\{1 - \tanh[(y - 1)/\xi]\}/2$ with $\xi = 0.2$, so that p decreases from $r^{1/2}$ to zero when y exceeds unity. Other expressions with this property also give oscillatory behavior. Figure 4 (b) shows the resulting time dependence of x and y in this homogeneous case ($D = 0$). Results are shown for oscillations in the limit cycle, with the phase adjusted to match the experiment. This qualitatively describes the observed behavior shown in Fig. 4(a). When the transport term is included, the model also produces propagating waves having similar patterns to those observed experimentally [23]. However, the predicted wave front shapes are significantly less sharp than those observed in the experiments, indicating that stronger nonlinearities are present in the real system than in this preliminary model. The width of the experimental InN-to-In wavefront is ~0.1 mm. Note that the 1.7-mm-long region illuminated by the x rays does not resolve this sharp wave front, so that its narrow width is not reflected in the x-ray data in Figs. 1 and 4.

The growth of InN by MOCVD represents a new type of excitable media involving bulk phase transitions. While many aspects of the nonlinear behavior observed correspond with those in other oscillating chemical systems (e.g. formation of propagating wave fronts, spirals, and chaotic patterns), the unique features of this system offer an opportunity to study new regimes of nonlinear chemical dynamics. Although for simplicity we have proposed a preliminary reaction-diffusion model similar to those developed for other oscillatory systems, there are several aspects of the metastable InN system that introduce additional nonlinear effects. The oscillating variables x and y are not the concentrations of molecules in solution or on a surface, but are the amounts of condensed-phase particles. Thus the relevant chemical activities are not expected to be linearly proportional to x and y, as is assumed in Eqs. (1) and (2). A more accurate model would take into account the nucleation of new particles and evolution of existing particles, the ratio of the particle surface area to volume determined by surface energies, etc. A multiscale approach that relates the macroscopic spatiotemporal oscillations to the underlying microscopic phase transition kinetics may provide a more revealing representation than the preliminary model developed here.

The observed oscillatory behavior also indicates the nature of the rate-limiting molecular processes occurring during synthesis of metastable nitrides. MOCVD growth of InN and (In,Ga)N has been found to depend in a complex manner on vapor composition such as V:III ratios [20,21]. The presence of InN or elemental In following deposition shows a surprising lack of correlation with $p(NH_3)$ [21]. Our interpretation of the oscillatory mechanism indicates that decomposition of NH_3 through heterogeneous catalysis at the substrate is the key process providing active nitrogen to form these metastable nitrides. Optimization of InN and (In,Ga)N growth processes will require not only understanding their dependences on the vapor phase composition but also tailoring the complex and time-dependent influence of the catalytic activity of the surface.

Experiments were performed at the Advanced Photon Source beam line 12ID-D. Work was supported under contract DE-AC-02-06CH11357 between UChicago Argonne, LLC, and the U. S. Department of Energy. K. R. E. was supported by NSF DMR-0413062.

*Present address: Department of Physics and Astronomy, Ohio University, Athens, OH 45701, USA.
†Present address: Numonyx, Santa Clara, CA 95054, USA.
‡stephenson@anl.gov

[1] B. A. Grzybowski *et al.*, Soft Matter **1**, 114 (2005).
[2] I. R. Epstein, J. A. Pojman, and O. Steinbock, Chaos **16**, 037101 (2006).
[3] A. S. Mikhailov and K. Showalter, Phys. Rep. **425**, 79 (2006).
[4] R. Imbihl and G. Ertl, Chem. Rev. **95**, 697 (1995).
[5] R. Imbihl, Catalysis Today **105**, 206 (2005).
[6] K. Krischer, in *Modern Aspects of Electrochemistry*, edited by B. E. Conway *et al.* (Kluwer Academic Plenum, New York, 1999), Vol. 32, p. 1.
[7] J. Christoph and M. Eiswirth, Chaos **12**, 215 (2002).
[8] C. B. Muratov, E. Vanden-Eijnden, and E. Weinan, Proc. Natl. Acad. Sci. U.S.A. **104**, 702 (2007).
[9] G. Bub, A. Shrier, and L. Glass, Phys. Rev. Lett. **94**, 028105 (2005).
[10] J.-S. Park *et al.*, Phys. Rev. Lett. **100**, 068302 (2008).
[11] T. Reichenbach, M. Mobilia, and E. Frey, Phys. Rev. Lett. **99**, 238105 (2007).
[12] J. H. E. Cartwright, R. Montagne, N. Piro, and O. Piro, Phys. Rev. Lett. **99**, 174101 (2007).
[13] O. U. Kheowan *et al.*, Phys. Rev. Lett. **98**, 074101 (2007).
[14] O. Rudzick and A. S. Mikhailov, Phys. Rev. Lett. **96**, 018302 (2006).
[15] L. Yang, I. Berenstein, and I. R. Epstein, Phys. Rev. Lett. **95**, 038303 (2005).
[16] A. G. Bhuiyan, A. Hashimoto, and A. Yamamoto, J. Appl. Phys. **94**, 2779 (2003).
[17] J. Wu *et al.*, Appl. Phys. Lett. **80**, 3967 (2002).
[18] C. A. Chang *et al.*, Phys. Status Solidi C **1**, 2559 (2004).
[19] O. Ambacher *et al.*, J. Vac. Sci. Technol. B **14**, 3532 (1996).
[20] B. Maleyre, O. Briot, and S. Ruffenach, J. Cryst. Growth **269**, 15 (2004).
[21] M. C. Johnson *et al.*, J. Cryst. Growth **272**, 400 (2004).
[22] G. B. Stephenson *et al.*, MRS Bull. **24** (1), 21 (1999).
[23] See EPAPS Document No. E-PRLTAO-101-072835 for methods, phase boundaries, details of model, and videos. For more information on EPAPS, see http://www.aip.org/pubservs/epaps.html.
[24] F. Jiang *et al.*, Appl. Phys. Lett. **89**, 161915 (2006).
[25] J. C. Ganley *et al.*, Catal. Lett. **96**, 117 (2004).